Dalton Transactions

ROYAL SOCIETY OF CHEMISTRY

PAPER

View Article Online
View Journal | View Issue

Cite this: *Dalton Trans.*, 2022, **51**, 3452

Synthesis, characterization and evaluation of aqueous Zn-based quantum dots for bioapplications†

Athina Papadopoulou, [a,b] Nikolaos Chalmpes,[c] Dimitrios Gournis, [c] Nikoleta Kostopoulou [a] and Eleni K. Efthimiadou *[a,b]

Received 26th November 2021,
Accepted 10th January 2022

DOI: 10.1039/d1dt04021a

rsc.li/dalton

Semiconducting nanoparticles called quantum dots (Qds) present unique optoelectronic properties based on their extremely small size, composition, and spherical shape, which make them suitable for use as diagnostic and theranostic agents in biological samples. The main scope of the fabrication of Qds is real-time diagnosis, therapy, drug delivery, and *in vitro* and *in vivo* tracking, presenting strong resistance to photobleaching. In this work, quantum dots such as ZnO, ZnSe, ZnS, and doped ZnS : Mn and ZnS : Cd were developed *via* a simple sol–gel synthesis in an aqueous solution. Morphological, structural, and optical characterizations were investigated. Moreover, *an in vitro* biological evaluation of Qds was performed. The results indicate that the photoluminescence is enhanced after doping ZnS Qds with Mn^{2+} and Cd^{2+}. Qds have been synthesized for use as fluorescent agents for real-time monitoring in bio-applications.

Introduction

Quantum dots are adjustable nanometer-sized semiconductors, luminescent nanocrystals, which have found significant applications in bioanalysis and bioimaging over the last few years. Some of their characteristics, such as brightness, photostability and size dependence, render them useful nanomaterials.[1] It is known that Qds have longer excited state lifetimes than organic dyes and resist photobleaching and chemical degradation.[2] The size dependence is due to quantum confinement. When the bulk semiconductors are reduced to the nanometer scale, the nanoparticles become smaller than the exciton radius, bringing about confinement of energy due to the electron–hole pair compression.[3] The pair electron–hole, which is attracted to each other by the electrostatic Coulomb force, is called an exciton (Fig. S1†). Consequently, the smaller the Qds synthesized the more compression of electron–hole pairs occurs, shifting to a higher energy level (blue shift), while larger Qds shift to lower energy levels (red shift), causing quantum effects on the material.[3–5]

The energy band gap increases when the diameter of the quantum dots is less than a certain value, which depends on the type of semiconductor. As a result, the energy band gap and, therefore, the optical properties of Qds can be adjusted according to their size.[6]

Many studies have focused on improving the photoluminescence stability of Qds, including different capping molecules.[7] The need for stable, monodispersed, and size-tunable Qds leads to the use of toxic chemicals, such as organometallic precursors and organic solvents. It is necessary to develop a new water-based methodology for preparing non-toxic and bio-friendly materials for bio-applications.[8–11]

Over the years, scientists have reported how impurities or dopants can affect nanocrystals by controlling their properties, especially their optical behaviour. An impurity with one or more valence electrons can provide extra electrons or holes. Consequently, these holes or electrons are available as carriers.[12]

This work introduces the production of zinc-based Qds using water as a solvent to decrease the use of toxic reagents in biosensor synthesis. Briefly, ZnO, ZnSe, and ZnS Qds doped with Mn^{2+} and Cd^{2+} were prepared presenting high photostability and overcome the limitations associated with photobleaching. The structural, morphological, and biological characterization of zinc-based Qds was performed to evaluate their theranostic applicability. For this reason, we evaluate the

[a]*Inorganic Chemistry Laboratory, Chemistry Department, National and Kapodistrian University of Athens, Panepistimiopolis, Zografou 157 71, Greece. E-mail: efthim@chem.uoa.gr, e.efthimiadou@inn.demokritos.gr; Tel: +30 210 7274858*
[b]*NCSR "Demokritos", Sol-Gel Laboratory, Institute of Nanoscience and Nanotechnology, 153 10 Aghia Paraskevi Attikis, Greece*
[c]*Department of Materials Science & Engineering, University of Ioannina, 45110 Ioannina, Greece*

†Electronic supplementary information (ESI) available. See DOI: 10.1039/d1dt04021a

potential of Qds in biological application, including MTT, wound healing assay, as well as fluorescence microscopy, for tracking in cells.

Experimental

Materials

Ethylene glycol (EG), hydrazine and (3-Mercaptopropyl) trimethoxysilane (MPTMS) were provided by Sigma-Aldrich. Diethanolamine (DEA), sodium sulfide, and cadmium acetate dihydrate were provided by Riedel-de Haën. Manganese(II) sulfate was provided by Acros Organics, and zinc salts (nitrate and acetate) were purchased from Alpha Aesar. Potassium hydroxide (KOH) was obtained from PanReac. Ethanol (EtOH) and distilled water were used as received in the experiments. Moreover, Poly-L-Lysine was provided by Merk and PBS, DMEM (high glucose), FBS (Fetal Bovine Serum), L-Glutamine and penicillin–streptomycin 100X were provided by Biosera. Dimethyl sulfoxide (DMSO) was purchased from Sigma Life Science and MTT was purchased from Cayman Chemical.

Characterization

UV/Vis spectra were obtained using a spectrometer (V-650, Jasco). The samples were prepared in distilled water. Photoluminescence was measured using a spectrometer (Horiba Jobin-Ybon iHR320, laser He–Cd (325 nm)). Scanning electron microscopy (SEM) using a Zeiss35 VP microscope with field emission electron gun (resolution 1.7 nm) 30 kV, coupled with an energy dispersive X-ray analyzer (EDX) for element

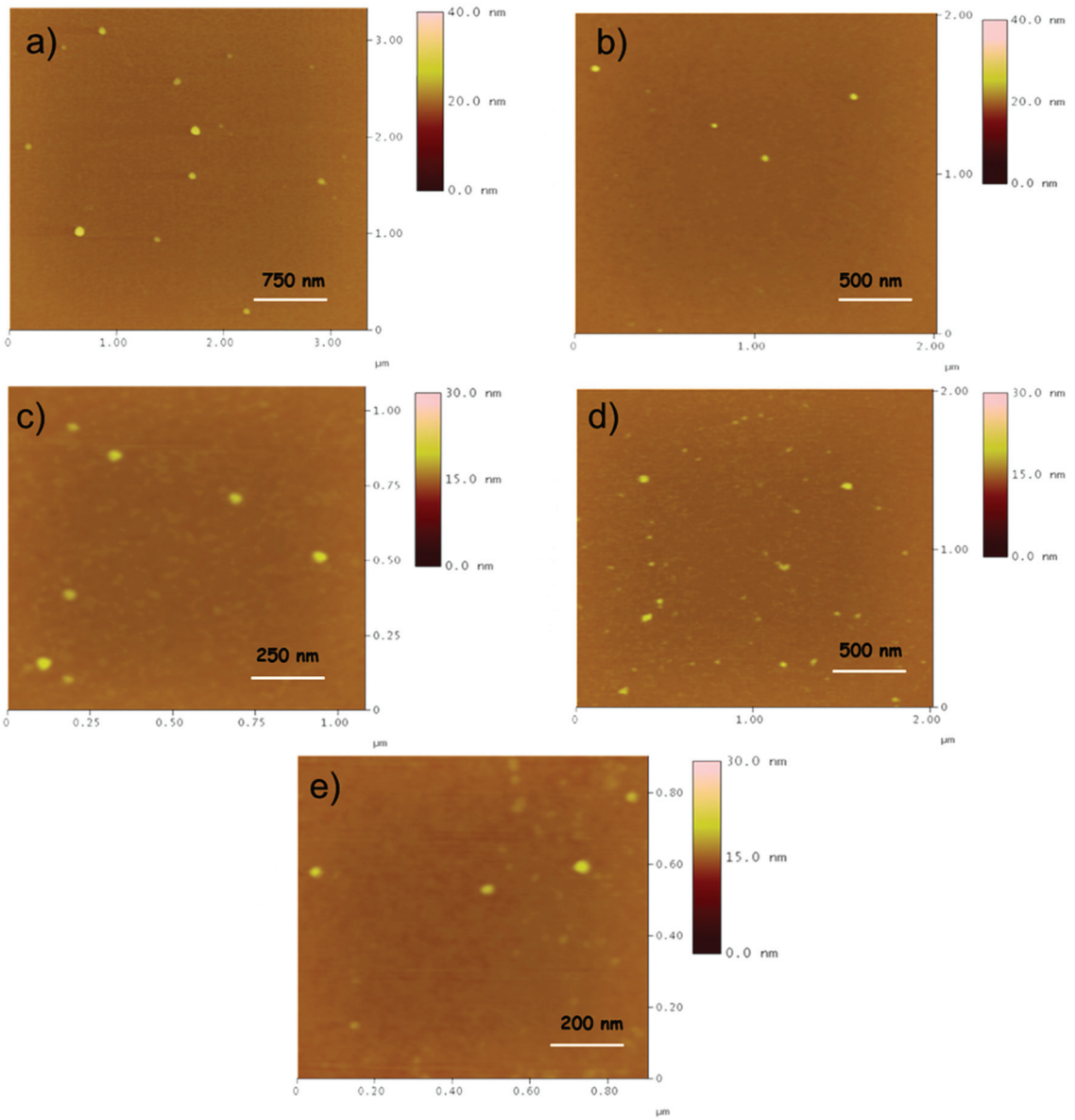

Fig. 1 AFM images of (a) ZnO, (b) ZnSe, (c) ZnS, (d) ZnS : Mn and (e) ZnS : Cd Qds.

analysis, using a Philips Quanta Inspect (FEI Company, Eindhoven, the Netherlands) microscope with a W (tungsten) filament 25 kV. X-ray diffraction measurements obtained with a Siemens D 500 powder X-Ray Diffractometer in the 2θ range of 10°–90° at a scan rate of 0.02° min^{-1}. DLS measurements were obtained using a spectrophotometer (Zetasizer Nanoseries, Malvern Instruments). Atomic force microscopy (AFM) images were collected in tapping mode with a Bruker Multimode 3D Nanoscope (Ted Pella Inc., Redding, CA, USA) using a micro-fabricated silicon cantilever type TAP-300G, with a tip radius of <10 nm and a force constant of approximately 20–75 N m^{-1}. Absorbance values of MTT were obtained using an ELISA Microplate Reader (Biobase – EL10A). In addition, images of quantum dots were captured using a fluorescence microscope (OMAX Trinocular Compound EPI, M834FLR).

Synthesis of ZnO Qds

Synthesis of ZnO Qds was based on the protocols of Ghorbani and Fu, with some modifications.[13,14] Zinc nitrate (37 mg, 0.124 mmol) was dissolved in 25 ml of distilled water, and then DEA (12.5 ml, 5 mM, 0.125 mmol) was added to the solution. In addition, 30 µl of OA was added to the mixture under vigorous stirring at room temperature. The temperature was increased to 90 °C for 2 h until the formation of Qds. A different synthetic route for ZnO QdS was the mixing of zinc nitrate (0.595 g, 0.2 M) and KOH (0.224 g, 0.4 M) in aqueous solution under continuous stirring at room temperature. The as-prepared solution was centrifuged at 5.000 rpm for 30 min and washed with ethanol. The product was then calcined at 600 °C for 5 h.

Table 1 *Z*-Range in nm of the synthesized Qds

Qds	*Z* Range (nm)
ZnO	7–11
ZnSe	4.2–6.5
ZnS	8
ZnS : Mn	6–10
ZnS : Cd	8

Synthesis of ZnSe Qds

Synthesis of ZnSe Qds was based on the work of Senthilkumar[15] with modifications. Zinc acetate (1.2 g, 5.4 mmol) was added to 100 ml of distilled water. EG (60 ml), hydrazine (40 ml), and elemental selenium (0.018 g) were added to the solution. The solution was refluxed overnight at 90 °C. The mixture was centrifuged and washed several times with ethanol, at 5.000 rpm for 5 min. The product was then dried at 50 °C for 6 h.

Synthesis of ZnS, ZnS : Mn and ZnS : Cd Qds

Synthesis of ZnS and ZnS doped with Mn^{2+} and Cd^{2+} Qds was based on the idea of Li and Bwatanglang,[16,17] with some modifications. Firstly, zinc nitrate (0.0605 g, 0.32 mmol), MPTMS (120 µl, 0.64 mmol), and Na_2S (209 µl, 5 mmol) were dissolved separately in deionized water in a sonic bath. The reagents were then added to 50 ml of water. The pH of the solution was fixed by adding tetramethylammonium hydroxide (TMAH). The solution was stirred overnight at 90 °C under N_2. The same synthesis was followed for ZnS Qds doped with Mn^{2+} and Cd^{2+}. Manganese(II) sulfate (0.033 g, 0.2 mmol) and cadmium acetate (0.053 g, 0.17 mmol) were added to the above solution to form ZnS : Mn and ZnS : Cd Qds, respectively. The pH of the solution in the case of ZnS, ZnS : Mn Qds was 12 and in the case of ZnS : Cd Qds was 8. The synthesis of ZnS : Mn Qds occurred at room temperature.

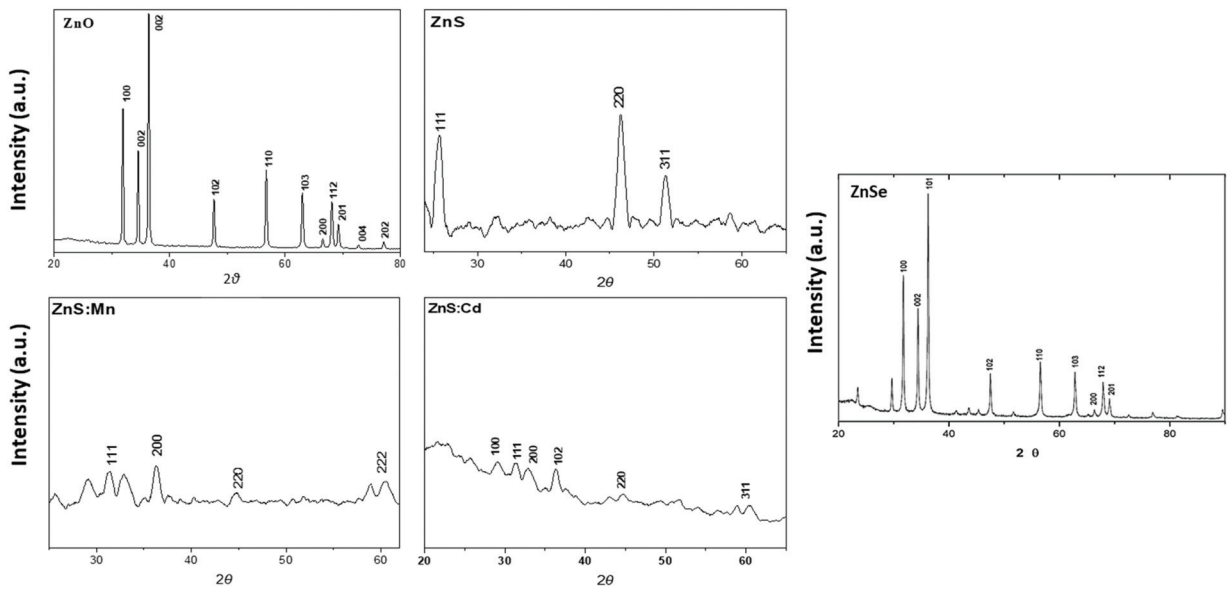

Fig. 2 X-ray diffraction (XRD) pattern of the ZnO, ZnS, ZnS : Mn, ZnS : Cd and ZnSe Qds.

Results and discussion

Morphological characterization

Atomic force microscopy (AFM). Qds' structure and morphology were investigated by atomic force microscopy (AFM). Representative AFM images deposited on a Si wafer by drop casting from aqueous dispersions are presented in Fig. 1, confirming the presence of spherical Qds. The size distribution of all nanostructures, as evaluated by AFM, was in the range of 4.2 to 11 nm. The exact sizes of each Qd are summarized in Table 1.

X-Ray diffraction analysis (XRD). The crystalline structure of Qds was studied by X-ray diffraction measurements obtained with a powder X-Ray Diffractometer 2θ range of 10°–90°, at a scan rate of 0.02° min^{-1}. The XRD pattern of the ZnO, ZnS, ZnS : Mn, ZnS : Cd and ZnSe which were prepared in aqua solution is shown in Fig. 2. All peaks can be indexed to ZnO wurtzite structure compared with the standard JCPDS (code no: 00-036-1451).[18] ZnS Qds at 2θ values match perfectly with the (111), (200), (220), (311), (400) and (331) crystalline planes of the face centered cubic structure compared with the standard JCPDS (code no: 65-1691). ZnSe X-ray diffraction pattern shows a characteristic pattern which corresponds to the (111), (200), (220) and (311) planes respectively matched with (cubic) zinc blende structure of ZnSe nanostructure (JCPDS code no: 37-1463 and 80-0021).[19,20] The XRD measurement of ZnS : Mn reveals that has Zinc blende structure, having planes (111), (200), (220) and (222). The cubic phase of the crystals is in agreement with standard JCPDS.[12] The peaks of ZnS : Cd show a cubic zinc blende structure, having planes (100), (111), (200), (102), (220) and (311).[12,21,22]

Energy dispersive X-Ray (EDAX). Quantitative elemental analysis of ZnO, ZnSe, ZnS, ZnS : Mn, and ZnS : Cd Qds was carried out using EDAX. In Fig. 3, the X-ray spectra for the qualitative analysis of Qds coincide with the AFM results. According to the results, we confirmed the presence of each element in Qds.

The chemical compositions of ZnO, ZnSe, ZnS, ZnS : Mn, and ZnS : Cd Qds were analyzed using EDX. The EDX patterns of nanoparticles are shown in Fig. 3 and the related data such as the wt% of Qds elements are listed in Table 2. The results verify the purity of nanoparticles.

Dynamic light scattering (DLS). The size of semiconductor nanocrystals in water was determined by DLS. A detailed analysis of the acquired DLS size and zeta is shown in Fig. 4, and the values are summarized in Table 3.

Table 2 Energy-dispersive X-ray spectroscopy (EDX) data of ZnO, ZnSe, ZnS, ZnS : Mn, ZnS : Cd nanoparticles

Qds	Element	wt%
ZnO	Zn	21.53
	O	78.46
	Total	100
ZnSe	Zn	47.05
	Se	52.94
	Total	100
ZnS	Zn	38.59
	S	61.40
	Total	100
ZnS : Mn	Zn	32.94
	S	48.52
	Mg	18.53
	Total	100
ZnS : Cd	Zn	20.60
	S	40.18
	Cd	39.21
	Total	100

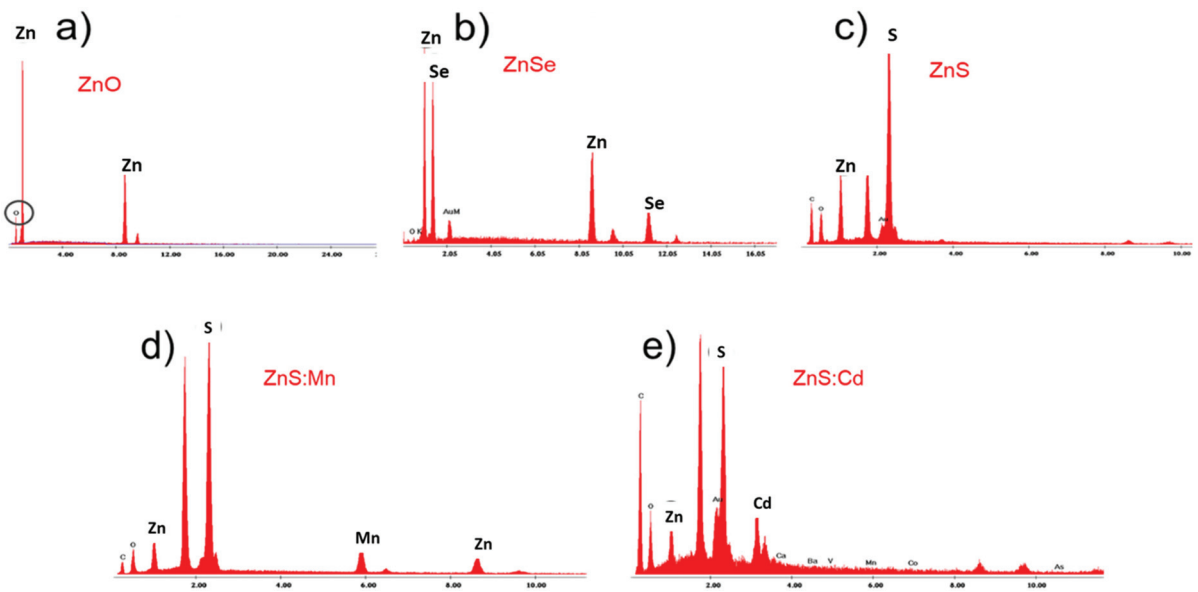

Fig. 3 X-ray spectra (EDAX) for qualitative analysis of (a) ZnO, (b) ZnSe, (c) ZnS, (d) ZnS : Mn, and (e) ZnS : Cd Qds.

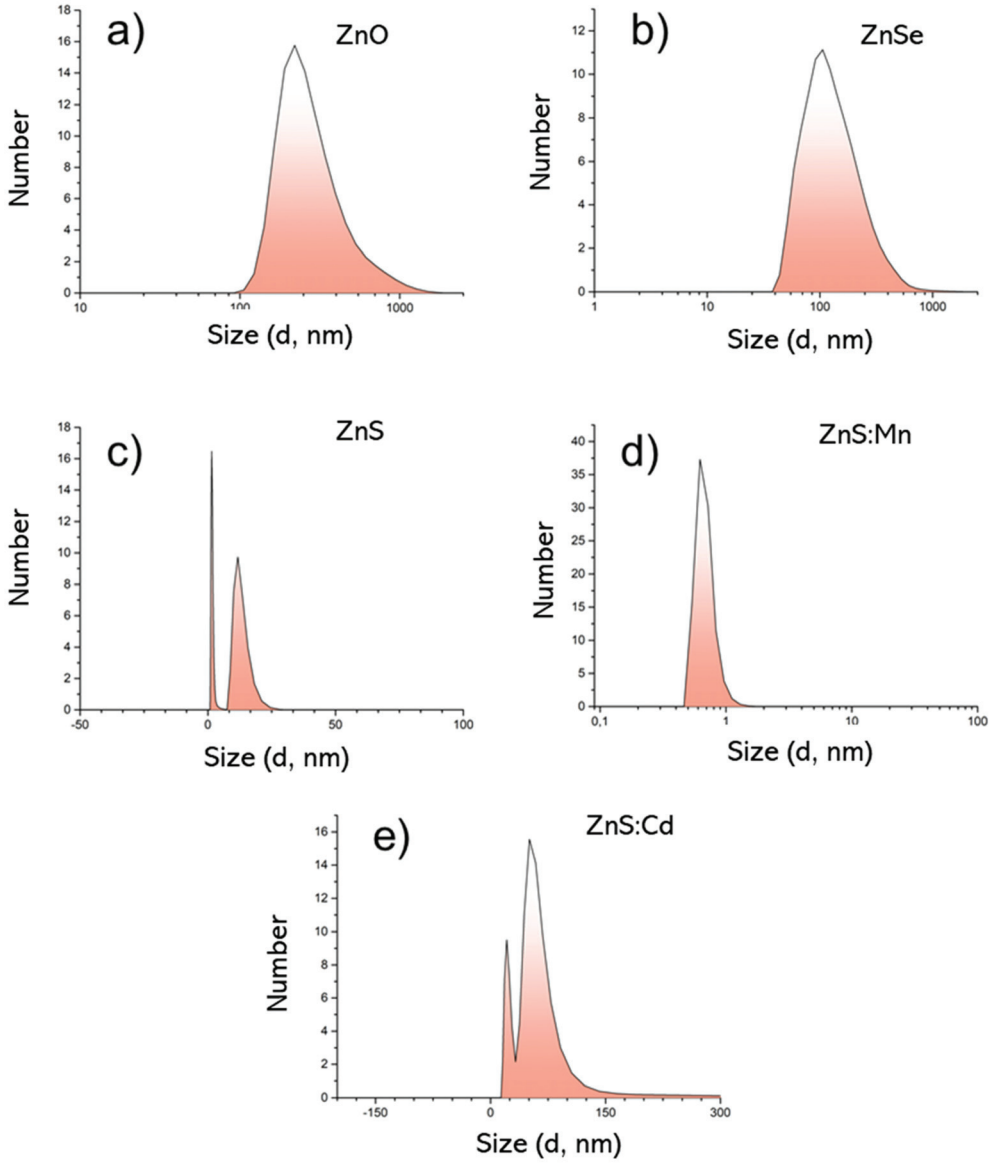

Fig. 4 DLS measurements by Number; (a) ZnO Qds, (b) ZnSe Qds, (c) ZnS Qds, (d) ZnS : Mn Qds and (e) ZnS : Cd Qds.

Based on the above-mentioned results (Fig. 4), the hydrodynamic diameter (Dh) is noticeably larger than the diameter in solid state, through AFM measurements. This increment can be attributed to the inter- and intra-molecular interactions of the $^{-}$OH groups of the metallic surfaces and also with water molecules. The zeta potential in all cases ranges between −13.7 mV and −45,9 mV supporting their excellent colloidal stability. Table 3 summarizes the size (Dh, nm) and zeta potential values, as well as the polydispersity index (PdI).

Optical properties. In the following comparative PL spectra of Qds (Fig. 5b), we observe an intensity enhancement of the ZnS emission peak after the enrichment of Qds with Cd^{2+}. Additionally, the comparative UV/Vis spectra of Qds (Fig. 5a) have a range of λ_{max} 247–270 nm. Tables 4 and 5 show λ_{max}, energies along with the Stokes shift of Qds. According to our PL measurements, a red shift was observed owing to the difference between the absorption and emission energies of Qds. This shift indicates lattice distortions and interface defects.[23,24]

In vitro biological evaluation

***In vitro* cytotoxicity study (MTT).** The cytotoxicity of Qds was evaluated *using* the MTT assay, an established colorimetric method. 3-(4,5-dimethylthiazol-2-yl)-2,5-diphenyl tetrazolium bromide (MTT) is a yellow tetrazole that can be reduced to purple formazan crystals in living cells by cellular reductase. A purple solution can be formed by the dilution of formazan crystals in DMSO. Solution absorbance was measured at 540 nm using a spectrometer (reference 620 nm).

Table 3 DLS data of size and zeta potential

Qds	Size (d, nm)	PdI	Zeta potential (mV)
ZnO	518.6	0.470	−21.8 ± 6.64
ZnSe	250	0.347	−37.6 ± 12.6
ZnS	93	0.629	−36.3
ZnS : Mn	779.6	0.648	−13.7 ± 8.59
ZnS : Cd	121	0.648	−45.9 ± 6.57

MCF-7 (breast cancer cells), HeLa (cervical cancer cells), and HEK 293 (human embryonic kidney cells) were used in this study. Cells were cultivated in Dulbecco's modified Eagle's medium (DMEM) supplemented with L-glutamine (2 mM), penicillin/streptomycin (100 U mL^{-1} penicillin, and 100 μg mL^{-1} streptomycin [PAA]), and 10% v/v fetal bovine serum at 37 °C in a 5% CO_2 atmosphere.[25]

The assay was performed in 96-well plates, and 10^4 cells were seeded per well and cultured for 24 h. Qds solutions were added (100 μl per well) in triplicates at five concentrations (100, 50, 25, 10 and 1 μM). After a 24 h incubation (37 °C, 5% CO_2, 95% air humidified atmosphere), the growth medium was removed and 100 μl of MTT solution in PBS (1 mg ml^{-1}) was added to each well. The cells were incubated further for 4 h to precipitate formazan crystals. DMSO (100 μl) was added to each well to dissolve the formazan crystals. Finally, absorbance was measured using an ELISA microplate reader (Biobase, EL10A). The results expressed as percentages of viability compared to the control are shown in Fig. 6. Qds, except for ZnSe, exhibited no significant cytotoxicity, even at the highest concentration of 100 μM after 24 h experiment.[26] ZnSe Qds are more toxic in both control and cancerous cells (60–80% toxicity) and this profile can be attributed to Se participation into nanocrystals. The other Qds observed almost 25% toxicity at 100 μM. It is worth mentioning that ZnS : Cd Qds do not express toxicity in all cell lines indicating that the Cd percentage in them, which is one of the most toxic metallic anion, do not affect the cell viability.

Wound healing assay. HeLa cells were treated with Qds and analyzed using a wound healing assay. Introducing an artificial scratch on a cell monolayer can provide information about the rate of wound closure, which indicates the speed of cell migration.[27] Cells were cultivated in Dulbecco's modified Eagle's medium (DMEM), which firstly prepared with L-glutamine (2 mM), penicillin/streptomycin (100 U mL^{-1} penicillin, and 100 μg mL^{-1} streptomycin [PAA]), and 10% v/v fetal bovine serum. Then the cultivation incubated at 37 °C in a 5% CO_2 atmosphere. The experiment was performed in 6 well plates, where cells were seeded and cultured until confluency. The wound area was calculated using the ImageJ software. The experiment was terminated after a 24 h healing process, when total closure in the control sample was observed. The wound area was calculated using the following equation:

$$\text{Wound healing } \% = (A_{\text{t-oh}} - A_{\text{t-xh}}/A_{\text{t-oh}}) \times 100.$$

where $A_{\text{t-0h}}$ is the measure of the initial wound area and $A_{\text{t-xh}}$ is the area of the wound measured x h after the scratch was made.[28]

In order to evaluate the toxic profile of our metallic Qds prepared using an eco-friendly methodology, we investigated the inhibition of wound closure by calculating indirectly the inhibition of cell proliferation and migration. HeLa cells were seeded in 6 well plate (one well served as a control) and 3 ml of culture medium were added after the wound was made using a sterilized tip. Moreover, 3 ml of culture medium in the presence of 100 μM Qds were introduced into the other wells.[29] The closure after 24 h of treatment with Zn-based Qds was found to be incomplete, in contrast to ZnS : Mn and ZnS : Cd (both are similar to the control experiment). The results presented in Fig. 7 and 8 lead to the conclusion that ZnSe QDs are more toxic than ZnS and ZnO, respectively. Other types of Qds were not toxic. These results were in agreement with the MTT assay results.

Fluorescence microscopy in cells. Cellular uptake of ZnO, ZnSe, ZnS, ZnS : Mn, and ZnS : Cd Qds was investigated using a fluorescence microscope (OMAX Trinocular Compound EPI, M834FLR model, 4x objective). HeLa cells were grown on 22 mm cover slips placed into six-well culture plates for 24 h, with 1.5 mL of culture medium. The cells were then incubated with the samples at 37 °C, in a 5% CO_2 atmosphere, for 1 h.

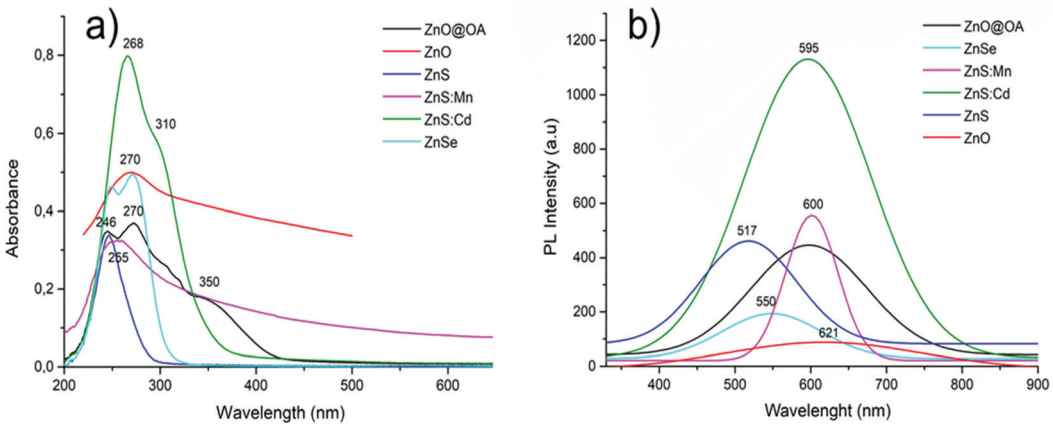

Fig. 5 Characterization of Qds, (a) UV/Vis spectra; (b) PL spectra of Qds.

Table 4 Absorption energy and λ_{max} of Qds

Qds	λ_{max} (nm)	$E_{absorption}$ (eV)
ZnO@OA	270	4.59
ZnO	270	4.59
ZnS	247	5.02
ZnS : Mn	255	4.86
ZnS : Cd	265	4.68
ZnSe	270	4.59

Table 5 Absorption Energy, λ_{max} and Stokes shift of Qds

Qds	λ_{max} (nm)	$E_{emission}$ (eV)	Stokes shift (eV)
ZnO@OA	597	2.07	2.52
ZnO	618	2	2.59
ZnS	517	2.4	2.62
ZnS : Mn	600	2.07	2.79
ZnS : Cd	595	2.09	2.59
ZnSe	548	2.26	2.33

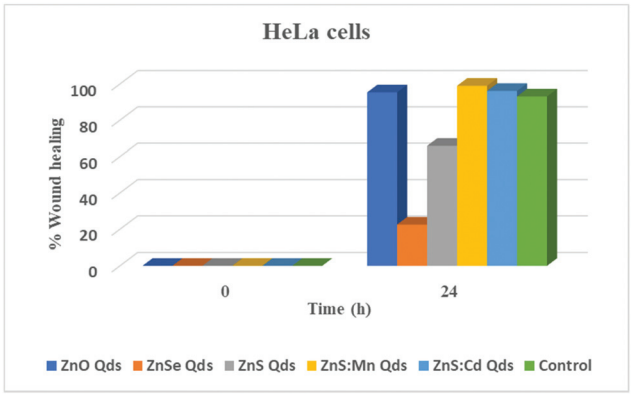

Fig. 7 Wound healing assay on HeLa cells treated with Qds at t = 0, 24 h.

The process followed was based on a standard protocol.[27,29] The cells were washed twice with PBS, fixed with 10% formaldehyde in PBS, and then coverslips were placed on microscope glass slides. Fluorescent images of Qds in the cells are shown in Fig. 9.

Cellular interactions with Qds were studied using HeLa cells after 1-hour incubation. According to the analysis, Qds showed different profiles of uptake and localization in the intracellular environment based on their composition. Zn is a common ingredient in Qds, and its fluorescent intensity (Fig. S2†), uptake, and localization is based on the combination of composed elements. As shown in Fig. 9, the fluorescent signal was detected on cell membrane, in the cytoplasm and perinuclear region, confirming the significant intracellular uptake of Qds. In detail, most of the detected Qds had diffuse cytoplasmic localization. Focusing on each Qd, we can see that cells incubated with ZnO and ZnS emit stronger fluorescent signals, indicating that higher concentrations are localized mainly on the cell membrane and internalized into the cytoplasm (Fig. 9b and d). ZnSe Qds were also observed in the cytoplasm and nucleus (Fig. 9c). ZnS : Mn and ZnS : Cd

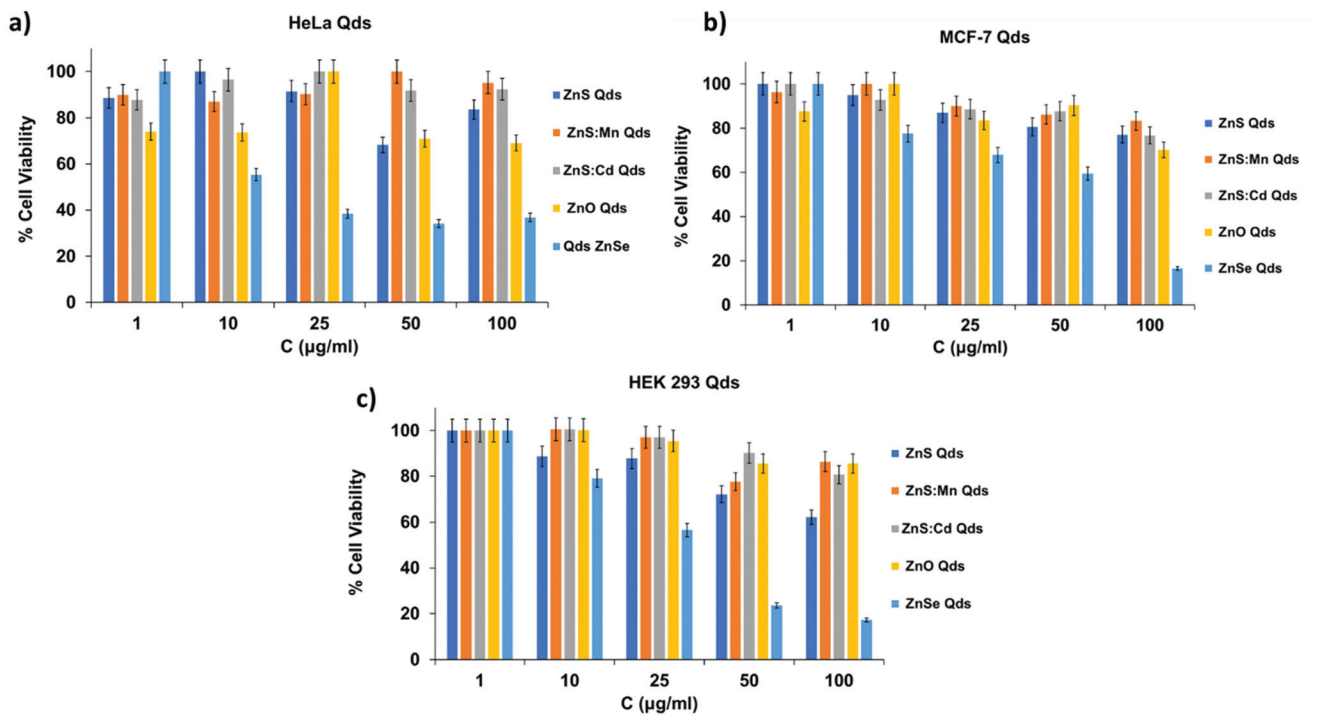

Fig. 6 MTT assay in cancer cells (a) MCF-7, (b) HeLa and control cells (c) HEK 293.

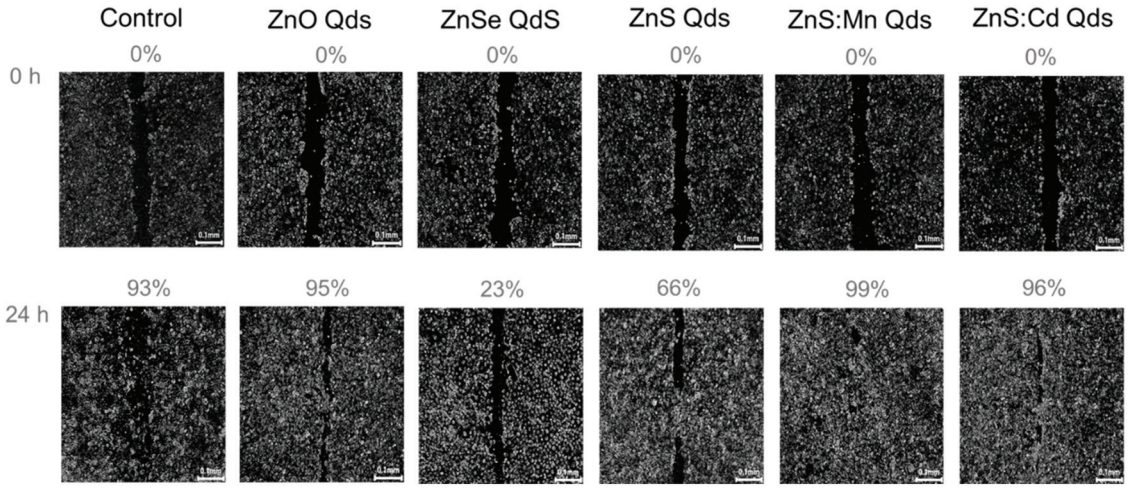

Fig. 8 Representative images for each experimental condition, at time points 0 h and 24 h after wound introduction, are presented (magnification ×20). Percentages indicate the wound closure. Scale bars correspond to 0.1 mm.

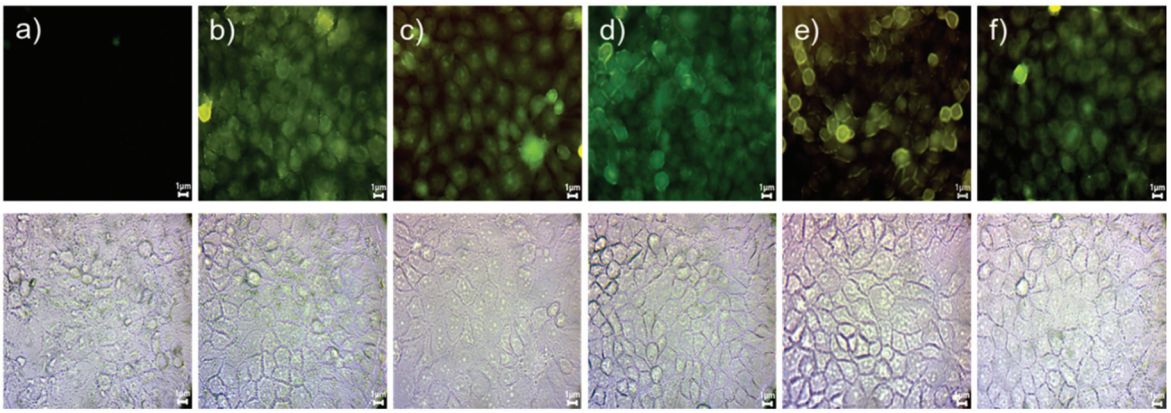

Fig. 9 Cellular uptake in HeLa cells treated with (a) control, (b) ZnO, (c) ZnSe, (d) ZnS, (e) ZnS : Mn and (f) ZnS : Cd Qds. Scale bars correspond to 1 μm.

were both observed in the cytoplasm, with the first exhibiting enhanced fluorescent properties (Fig. 9e and f).

Conclusion

In conclusion, we synthesized Zn-based Qds doped with Cd^{2+} and Mn^{2+}, improving their fluorescence properties for *in vitro* and *in vivo* applications. First, Qds synthesized in aqueous solutions decrease the use of toxic materials in biosensor synthesis. The structure and morphology of Qds were determined by atomic force microscopy (AFM), confirming the presence of spherical Qds. In addition, the purity and crystallinity of Qds were determined by XRD analysis. The chemical compositions of them were analyzed using EDX. The size distribution of all nanostructures, as evaluated by AFM, was 4.2–11 nm.

Cytotoxicity of Qds was estimated using the MTT assay. HeLa, MCF-7, and HEK 293 cell lines were treated with Qds for 24 h and the results are expressed as the percentage viability of the cells. A wound healing assay was used to determine the inhibition of cell proliferation and migration indirectly. ZnSe Qds were found to be more toxic than ZnS and ZnO. Other types of Qds were not toxic. *In vitro* uptake characteristics of Qds in HeLa cells were studied using fluorescence microscopy. *In vitro* studies have shown non-specific cellular uptake and localization. According to our results, regarding the physicochemical and internalization properties of Qds, we strongly suggest that Qds can evolve into an important tool for biomedical and therapeutic applications.

Statements

All methods were carried out in accordance with relevant guidelines and regulations.

All experimental protocols do not need to be approved by the institute. The informed consent was obtained from all subjects and/or their legal guardian(s).

All experiments with cell cultures and discarded blood from unknown patient approval is not necessary.

Data access statement

All relevant data are within the paper and its ESI.†

Conflicts of interest

There are no conflicts to declare.

Acknowledgements

This work was financially supported by the Special Research Account (SARG) of the National and Kapodistrian University of Athens (15244, 16672). We acknowledge support of this work by the project "National Infrastructure in Nanotechnology, Advanced Materials and Micro-/Nanoelectronics" (MIS-5002772) which is implemented under the Action "Reinforcement of the Research and Innovation Infrastructure", funded by the Operational Programme "Competitiveness, Entrepreneurship and Innovation" (NSRF 2014-2020) and co-financed by Greece and the European Union (European Regional Development Fund).

References

1 B. A. Kairdolf, A. M. Smith, T. H. Stokes, M. D. Wang, A. N. Young and S. Nie, Semiconductor Quantum Dots for Bioimaging and Biodiagnostic Applications, *Annu. Rev. Anal. Chem.*, 2013, **6**, 143–162, DOI: 10.1146/annurev-anchem-060908-155136.

2 Y. Yin and A. P. Alivisatos, Colloidal nanocrystal synthesis and the organic-inorganic interface, *Nature*, 2005, **437**, 664–670, DOI: 10.1038/nature04165.

3 V. G. Reshma and P. V. Mohanan, Quantum dots: Applications and safety consequences, *J. Lumin.*, 2019, **205**, 287–298, DOI: 10.1016/j.jlumin.2018.09.015.

4 C. De Mello Donegá, *Nanoparticles: Workhorses of nanoscience*, 2014. DOI: 10.1007/978-3-662-44823-6.

5 D. Sumanth Kumar, B. Jai Kumar and H. M. Mahesh, *Quantum Nanostructures (QDs): An Overview*, Elsevier Ltd., 2018. DOI: 10.1016/b978-0-08-101975-7.00003-8.

6 Z. Yu, H. Lv and D. Tang, One pot synthesis of water stable ZnO quantum dots with binding ability to microbe, *Mater. Lett.*, 2018, **210**, 207–210, DOI: 10.1016/j.matlet.2017.09.036.

7 C. Carrillo-Carrión, S. Cárdenas, B. M. Simonet and M. Valcárcel, Quantum dots luminescence enhancement due to illumination with UV/Vis light, *Chem. Commun.*, 2009, 5214–5226, DOI: 10.1039/b904381k.

8 X. Peng, Green chemical approaches toward high-quality semiconductor nanocrystals, *Chem. – Eur. J.*, 2002, **8**, 334–339, DOI: 10.1002/1521-3765(20020118)8:2<334::aid-chem334>3.0.co;2-t.

9 D. Bera, L. Qian, T. K. Tseng and P. H. Holloway, Quantum dots and their multimodal applications: A review, *Materials*, 2010, **3**, 2260–2345, DOI: 10.3390/ma3042260.

10 S. J. Rosenthal, J. C. Chang, O. Kovtun, J. R. McBride and I. D. Tomlinson, Biocompatible quantum dots for biological applications, *Chem. Biol.*, 2011, **18**, 10–24, DOI: 10.1016/j.chembiol.2010.11.013.

11 E. Petryayeva, W. R. Algar and I. L. Medintz, Quantum dots in bioanalysis: A review of applications across various platforms for fluorescence spectroscopy and imaging, *Appl. Spectrosc.*, 2013, **67**, 215–252, DOI: 10.1366/12-06948.

12 D. J. Norris, A. L. Efros and S. C. Erwin, Doped nanocrystals, *Science*, 2008, **319**, 1776–1779, DOI: 10.1126/science.1143802.

13 H. R. Ghorbani, F. P. Mehr, H. Pazoki and B. M. Rahmani, Synthesis of ZnO nanoparticles by precipitation method, *Orient. J. Chem.*, 2015, **31**, 1219–1221, DOI: 10.13005/ojc/310281.

14 Y. S. Fu, X. W. Du, S. A. Kulinich, J. S. Qiu, W. J. Qin, R. Li, J. Sun and J. Liu, Stable aqueous dispersion of ZnO quantum dots with strong blue emission via simple solution route, *J. Am. Chem. Soc.*, 2007, **129**, 16029–16033, DOI: 10.1021/ja075604i.

15 K. Senthilkumar, T. Kalaivani, S. Kanagesan and V. Balasubramanian, Synthesis and characterization studies of ZnSe quantum dots, *J. Mater. Sci.: Mater. Electron.*, 2012, **23**, 2048–2052, DOI: 10.1007/s10854-012-0701-1.

16 I. B. Bwatanglang, F. Mohammad, N. A. Yusof, J. Abdullah, M. Z. Hussein, N. B. Alitheen and N. Abu, Folic acid targeted Mn:ZnS quantum dots for theranostic applications of cancer cell imaging and therapy, *Int. J. Nanomed.*, 2016, **11**, 413–428, DOI: 10.2147/IJN.S90198.

17 H. Li, W. Y. Shih and W. H. Shih, Non-heavy-metal ZnS quantum dots with bright blue photoluminescence by a one-step aqueous synthesis, *Nanotechnology*, 2007, **18**, 205604–205611, DOI: 10.1088/0957-4484/18/20/205604.

18 Z. M. Xu, J. Lu, Z. M. Ao and S. Li, A New Preparation Method to Significantly Improve the Photocatalytic Activity of ZnO Nanoparticles, *Th Annu. Condens. Matter Mater.*, 2014, pp. 1–5.

19 G. Bakiyaraj and R. Dhanasekaran, Synthesis and characterization of flower-like ZnSe nanostructured thin films by chemical bath deposition (CBD) method, *Appl. Nanosci.*, 2013, **3**, 125–131, DOI: 10.1007/s13204-012-0075-y.

20 R. Indirajith, M. Rajalakshmi, K. Ramamurthi, M. B. Ahamed and R. Gopalakrishnan, Synthesis of ZnSe nano particles, deposition of ZnSe thin films by electron beam evaporation and their characterization, *Ferroelectrics*, 2014, **467**, 13–21, DOI: 10.1080/00150193.2014.874892.

21 A. Khorsand Zak, R. Razali, W. H. Abd Majid and M. Darroudi, Synthesis and characterization of a narrow size distribution of zinc oxide nanoparticles, *Int. J. Nanomed.*, 2011, **6**, 1399–1403, DOI: 10.2147/ijn.s19693.

22 N. Soltani, E. Saion, M. Z. Hussein, M. Erfani, A. Abedini, G. Bahmanrokh, M. Navasery and P. Vaziri, Visible light-induced degradation of methylene blue in the presence of photocatalytic ZnS and CdS nanoparticles, *Int. J. Mol. Sci.*, 2012, **13**, 12242–12258, DOI: 10.3390/ijms131012242.

23 D. Sun, H. J. Sue and N. Miyatake, Optical properties of ZnO quantum dots in epoxy with controlled dispersion, *J. Phys. Chem. C*, 2008, **112**, 16002–16010, DOI: 10.1021/jp805104h.

24 J. G. Lu, Z. Z. Ye, Y. Z. Zhang, Q. L. Liang, S. Fujita and Z. L. Wang, Self-assembled ZnO quantum dots with tunable optical properties, *Appl. Phys. Lett.*, 2006, **89**, 2–5, DOI: 10.1063/1.2221892.

25 A. F. Metaxa, E. K. Efthimiadou, N. Boukos, E. A. Fragogeorgi, G. Loudos and G. Kordas, Hollow microspheres based on - Folic acid modified - Hydroxypropyl Cellulose and synthetic multi-responsive bio-copolymer for targeted cancer therapy: Controlled release of daunorubicin, in vitro and in vivo studies, *J. Colloid Interface Sci.*, 2014, **435**, 171–181, DOI: 10.1016/j.jcis.2014.08.001.

26 T. S. Koutsikou, M. G. Krokidis, N. Boukos, G. Mitrikas and E. Efthimiadou, Synthesis, characterization and evaluation of multi sensitive nanocarriers by using the layer by layer method, *J. Drug Delivery Sci. Technol.*, 2019, **53**, 101142, DOI: 10.1016/j.jddst.2019.101142.

27 J. E. N. Jonkman, J. A. Cathcart, F. Xu, M. E. Bartolini, J. E. Amon, K. M. Stevens and P. Colarusso, An introduction to the wound healing assay using live-cell microscopy, *Cell Adhes. Migr.*, 2014, **8**, 440–451, DOI: 10.4161/cam.36224.

28 A. Grada, M. Otero-Vinas, F. Prieto-Castrillo, Z. Obagi and V. Falanga, Research Techniques Made Simple: Analysis of Collective Cell Migration Using the Wound Healing Assay, *J. Invest. Dermatol.*, 2017, **137**, e11–e16, DOI: 10.1016/j.jid.2016.11.020.

29 M. Theodosiou, N. Boukos, E. Sakellis, M. Zachariadis and E. K. Efthimiadou, Gold nanoparticle decorated pH-sensitive polymeric nanocontainers as a potential theranostic agent, *Colloids Surf., B*, 2019, **183**, 110420, DOI: 10.1016/j.colsurfb.2019.110420.